# Electronic Supplementary Information

# Rapid synthesis of fault-free GME zeolite

Jingqiu Li,[a,b] Caiping Sheng,[b] Ye Ma,[c] Liangni Ban,[b] Jie Zhu,[b] Zhongping Huang,*[,a] Hongxia Shen,[b] Xuebo Cao*[,b] and Longfeng Zhu*[,b]

[a] College of Chemical Engineering, Zhejiang University of Technology, Hangzhou 310014, China.

[b] College of Biological, Chemical Science and Engineering, Jiaxing University, Jiaxing 314001, China.

[c] School of Physical Science and Technology & Shanghai Key Laboratory of High-resolution Electron Microscopy, ShanghaiTech University, Shanghai 201210, China.

*Corresponding author. E-mail: zphuang@zjut.edu.cn; xbcao@zjxu.edu.cn; zhulf1988@mail.zjxu.edu.cn

**Materials**

Silica sol ($SiO_2$, 30%, Zhejiang Yuda Chemical Co., Ltd.), sodium aluminate ($NaAlO_2$, CP, Sinopharm Chemical Reagent Co., Ltd.), sodium hydroxide (NaOH, 96%, Aladdin Chemistry Co., Ltd.), N,N-dimethyl-3,5-dimethylpiperidinium hydroxide ($C_9H_{21}NO$, 25%, Kente Catalysts Inc.), potassium chloride (KCl, AR, Aladdin Chemistry Co., Ltd.), sodium chloride (NaCl, AR, Zhejiang Chemical Reagent Co., Ltd.). The deionized water was made in laboratory.

**Characterization**

XRD patterns of the samples were collected with a Shimadzu MAXima XRD-7000 X-ray diffractometer (40 kV, 40 mA) using Cu Kα radiation (λ = 1.5406 Å) with a flat-plate sample holder. Scanning electron microscopy (SEM) images of the samples were performed on Hitachi SU1510 and Thermo Scientific Apreo S HiVac field emission scanning electron microscopes. $N_2$ sorption experiments of the samples were performed on a Micromeritics ASAP 2020M. The pore volume and surface area were calculated by using the t-plot and Brunauer-Emmett-Teller (BET) methods. Thermogravimetric-differential thermal analysis (TG-DTA) was performed on a PerkinElmer TGA 7 analyzer from 22 to 1000 °C with a heating rate of 10 °C $min^{-1}$. The GME zeolite composition was determined by X-ray Fluorescence (XRF) with an EDX-7000 spectrometer and inductively coupled plasma optical emission spectrometer (ICP-OES) with a Perkin-Elmer 3300DV emission spectrometer. Fourier transform infrared (FTIR) spectra were obtained using an Agilent 640 instrument equipped with a KBr beam splitter. The data were collected within the frequency region of 4000-2500 $cm^{-1}$ with a resolution of 4 $cm^{-1}$. Solid-state NMR spectra of the samples were recorded on an AVANCE NEO 600M spectrometer. Liquid NMR spectra were recorded on a Varian 400MR spectrometer using a 5 mm QNP probe equipped with z-gradient coil. Transmission Electron Microscope (TEM) JEM-F200 is operating at an acceleration voltage of 200 kV and the selected area electron diffraction (SAED) pattern and high-resolution transmission electron microscopy (HRTEM) image was

collected at the same time.

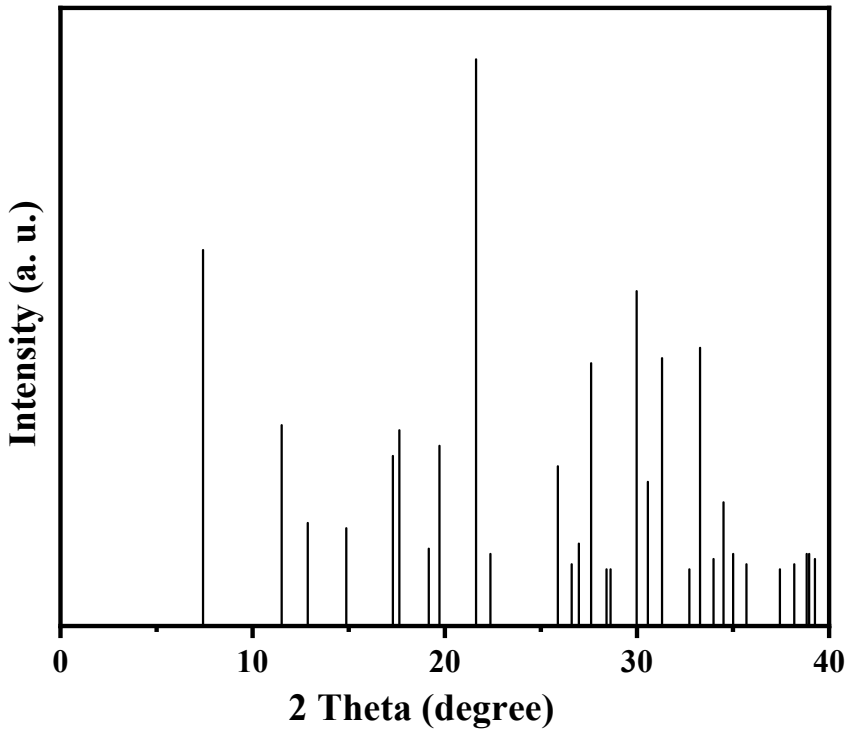


**Fig. S1.** The simulated XRD pattern of GME structure.

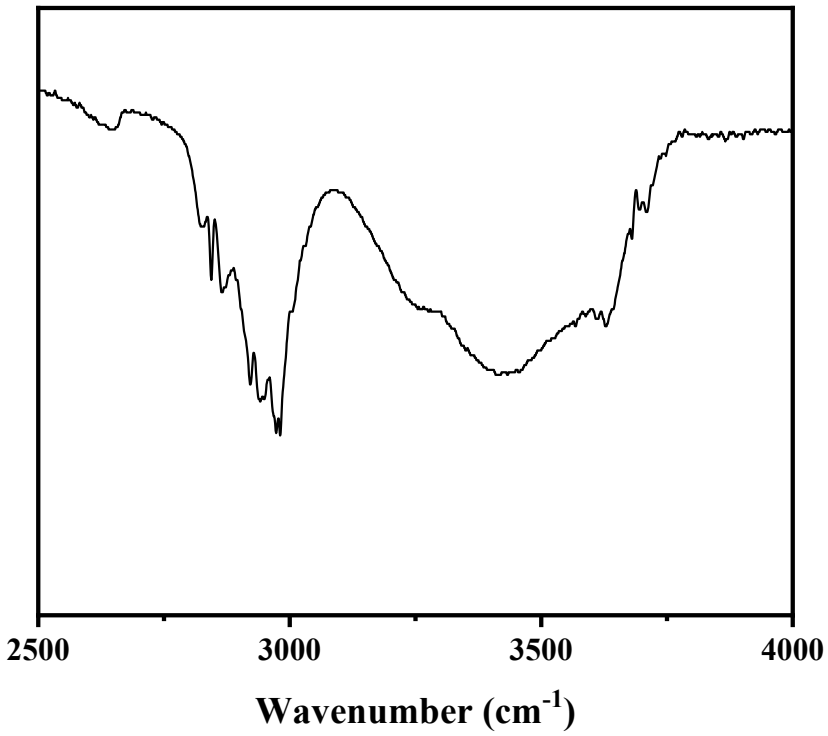


**Fig. S2.** The FTIR spectrum of GME zeolite.

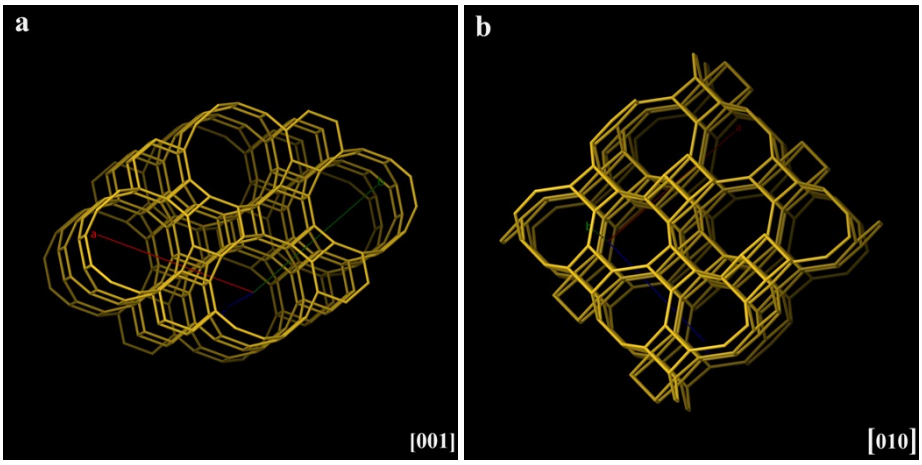


**Fig. S3.** The framework images of GME zeolite viewed from different direction.

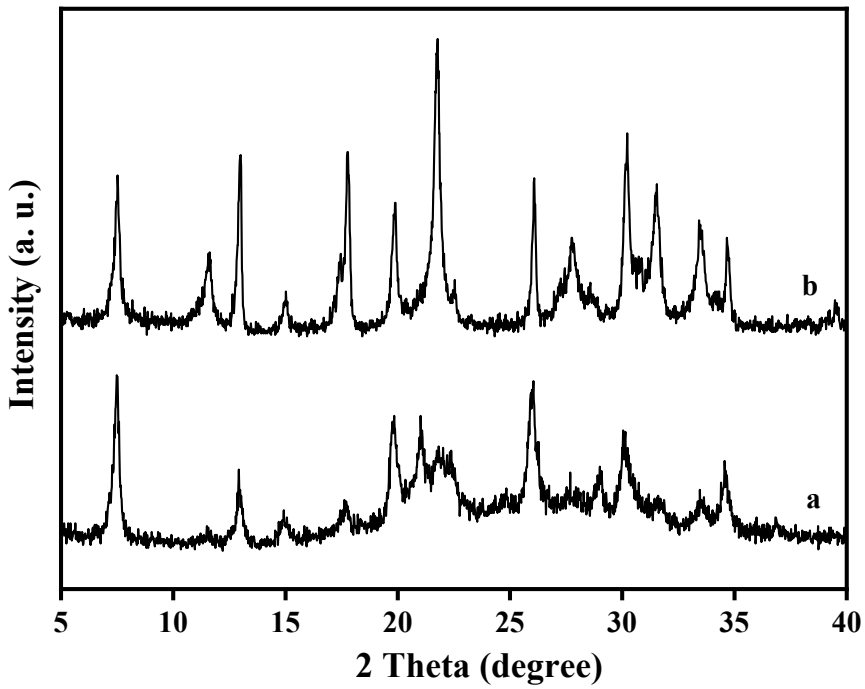


**Fig. S4.** XRD patterns of directly calcined (a) and KS-GME (b) zeolite product.

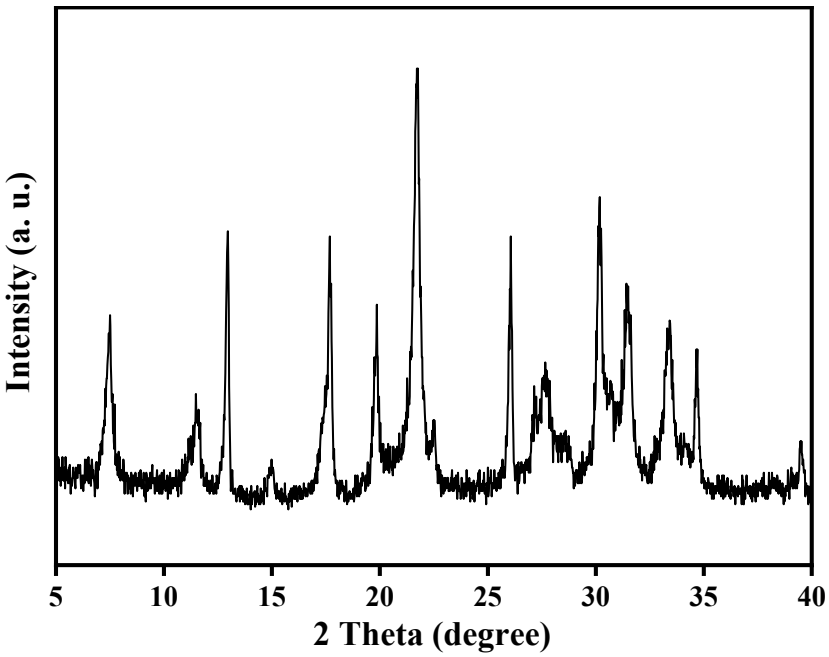


**Fig. S5.** XRD pattern of K-GME zeolite.

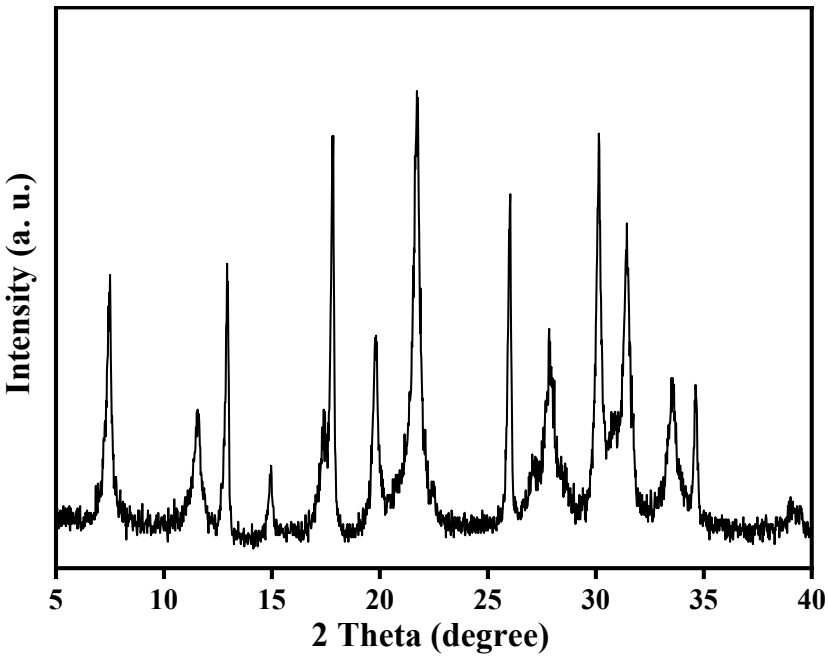


**Fig. S6.** XRD pattern of Na-GME zeolite.

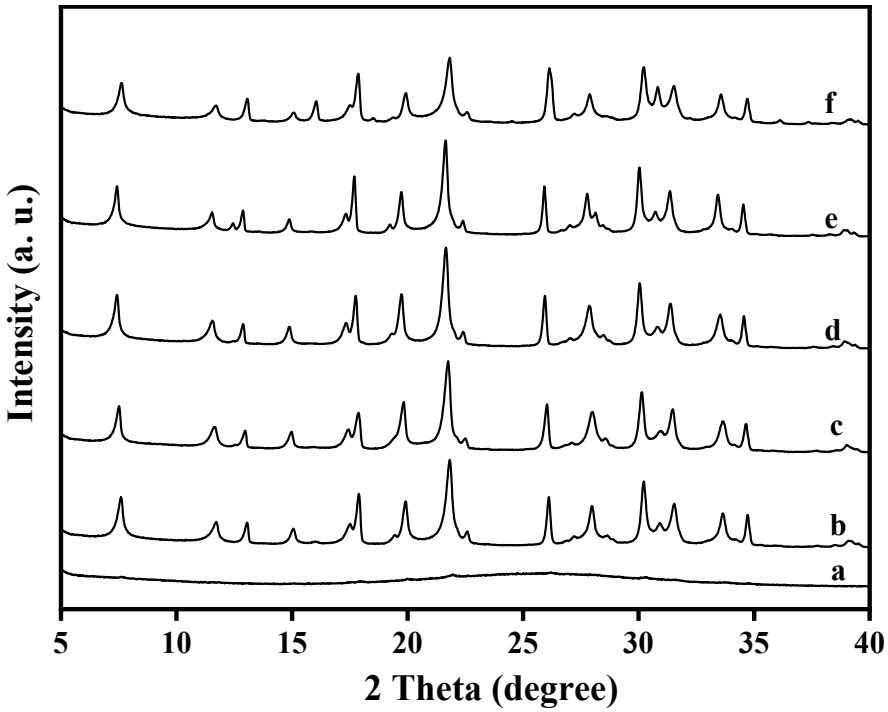


**Fig. S7.** XRD patterns of the products synthesized with $Na_2O/SiO_2$ ratios at (a) 0.25, (b) 0.28, (c) 0.31, (d) 0.34, (e) 0.37 and (f) 0.40. The products were synthesized at 160 °C for 4 h.

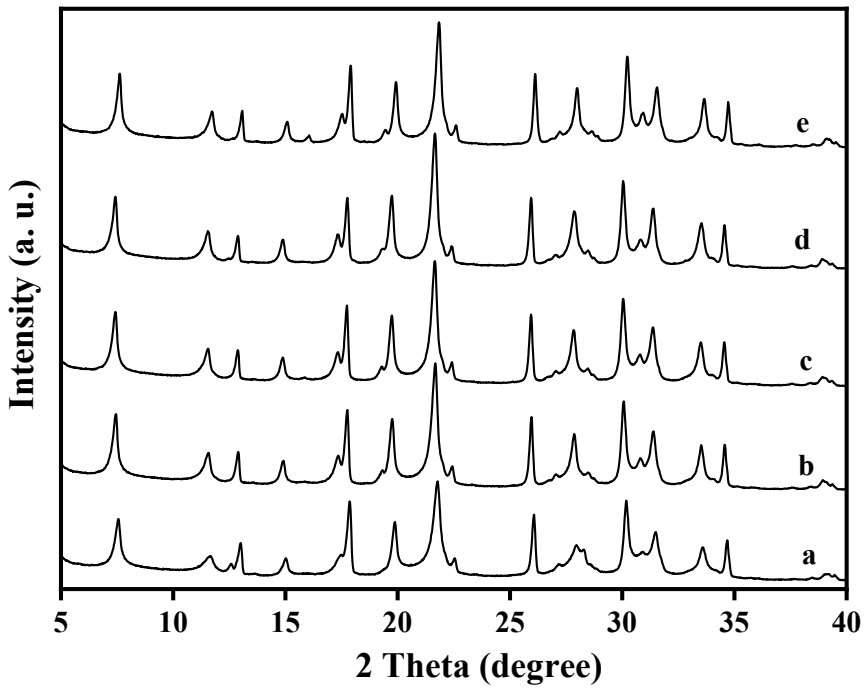


**Fig. S8.** XRD patterns of the products synthesized with OSDA/$SiO_2$ ratios at (a) 0.076, (b) 0.096, (c) 0.116, (d) 0.136, and (e) 0.156. The products were synthesized at 160 °C for 4 h.

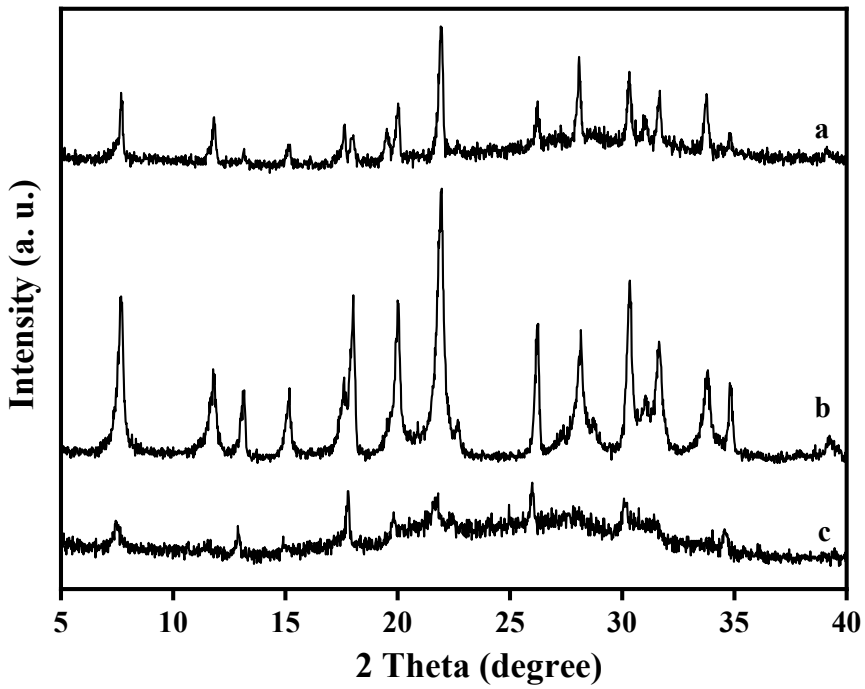


**Fig. S9.** XRD patterns of the products synthesized with $H_2O/SiO_2$ ratios at (a) 5, (b) 15, and (c) 30. The products were synthesized at 160 °C for 4 h.

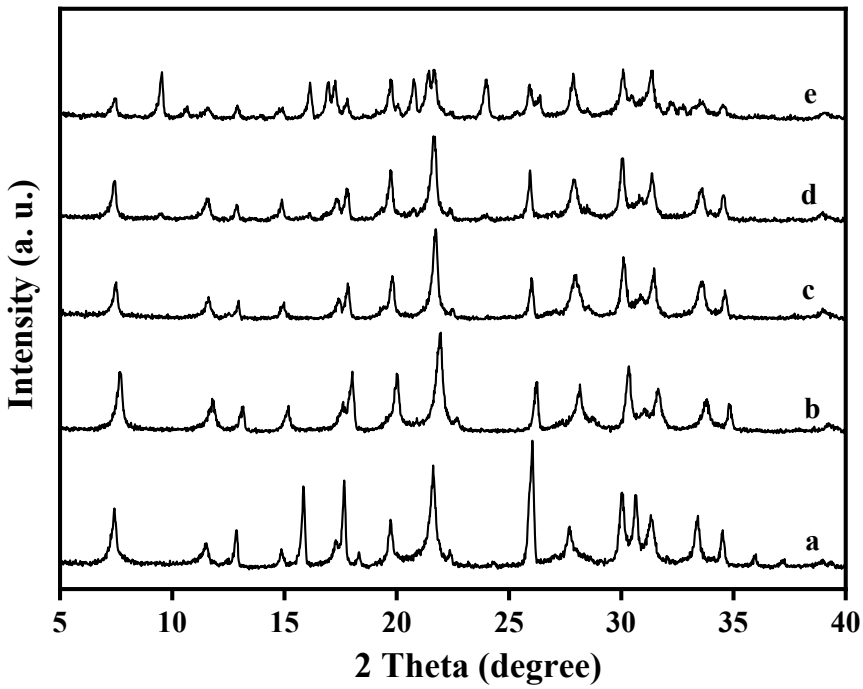


**Fig. S10.** XRD patterns of the products synthesized with Si/Al ratios at (a) 10, (b) 20, (c) 40, (d) 60 and (e) 80. The products were synthesized at 160 °C for 4 h.

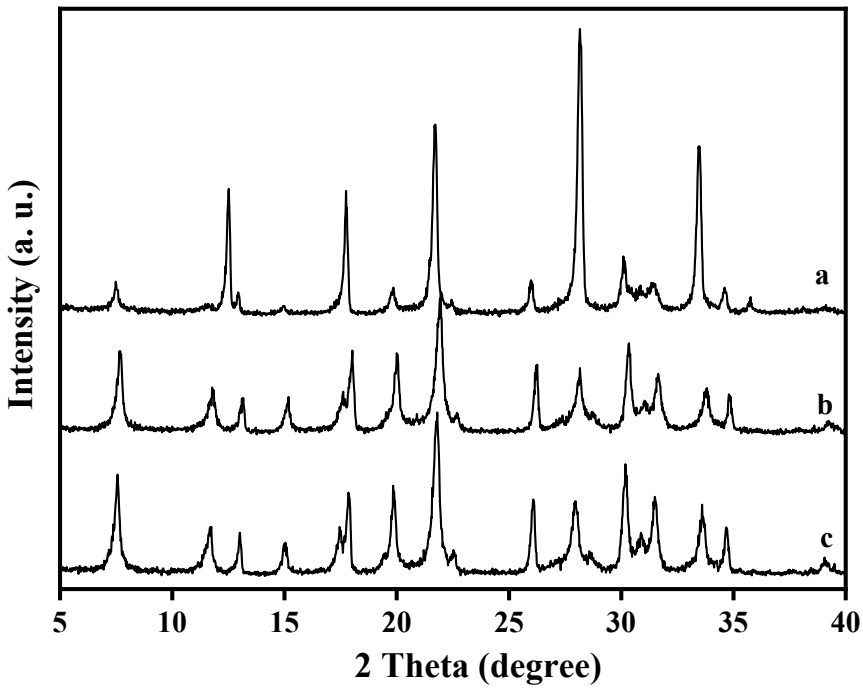


**Fig. S11.** XRD patterns of the products synthesized with seeds amount at (a) 0, (b) 2 and (c) 4%. The products were synthesized at 160 °C for 4 h.

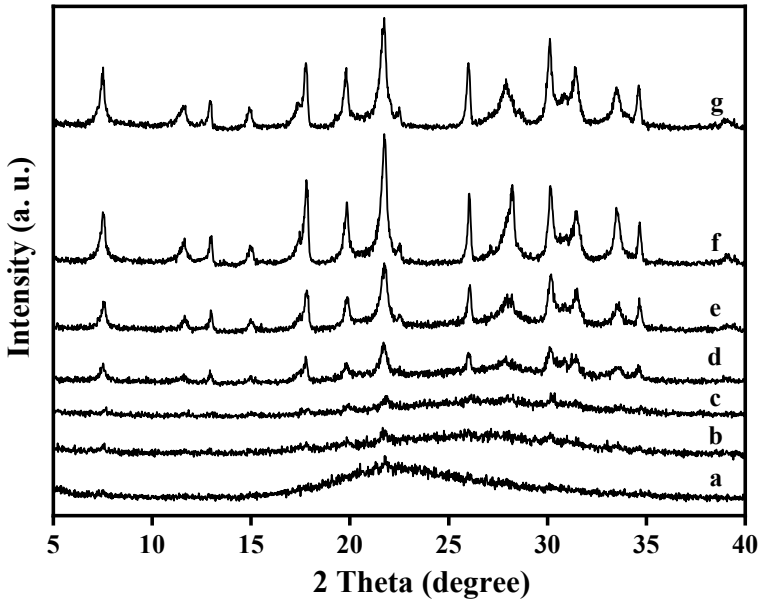


**Fig. S12.** XRD patterns of the GME zeolite crystallized at 140 °C for (a) 0, (b) 1, (c) 2, (d) 3, (e) 4, (f) 6 h and (g) 8 h.

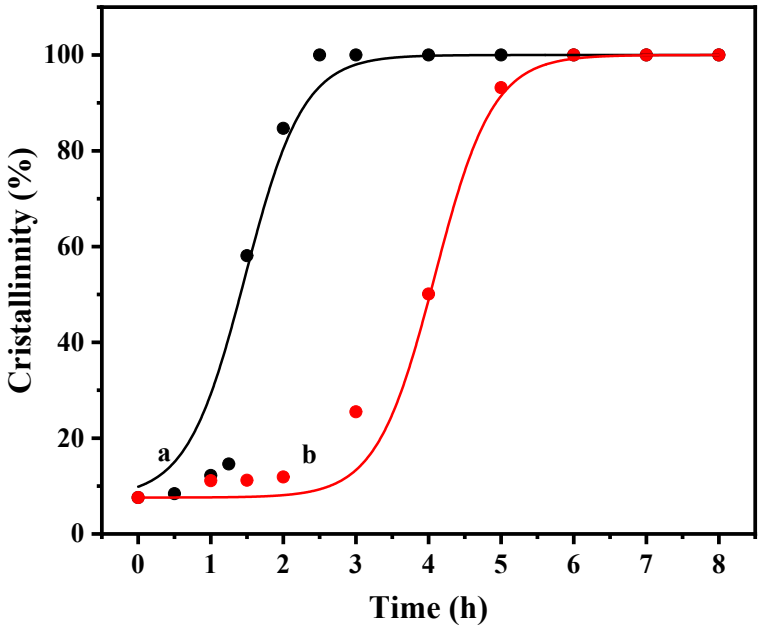


**Fig. S13.** The dependence of the GME zeolites crystallinity on the crystallization time at 160 °C (a) and 140 °C (b).

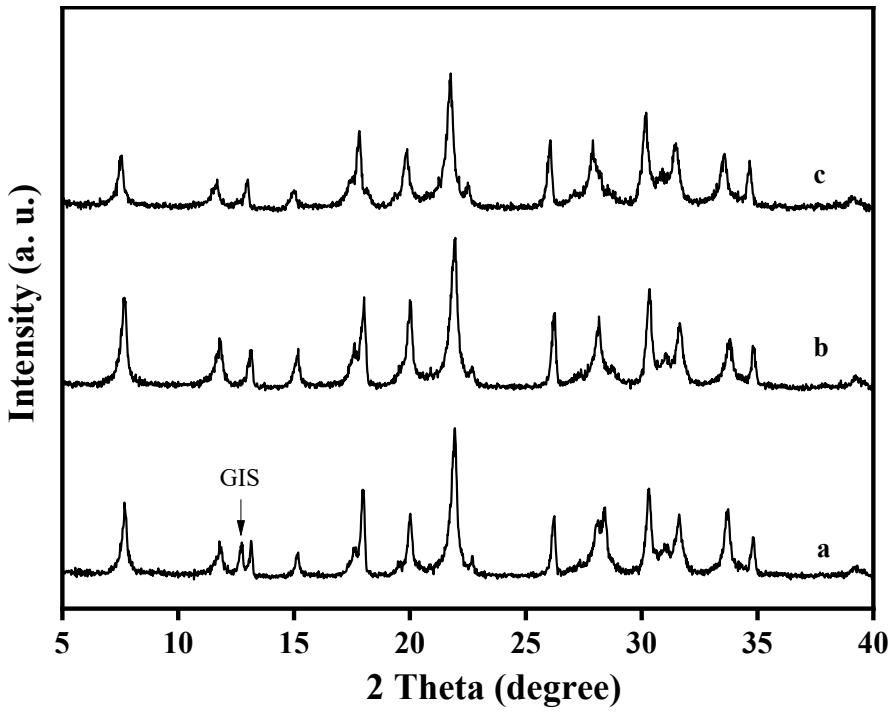


**Fig. S14.** XRD patterns of the products synthesized with aging time at (a) 10 min, (b) 3 h and (c) 12 h after addition of seed.

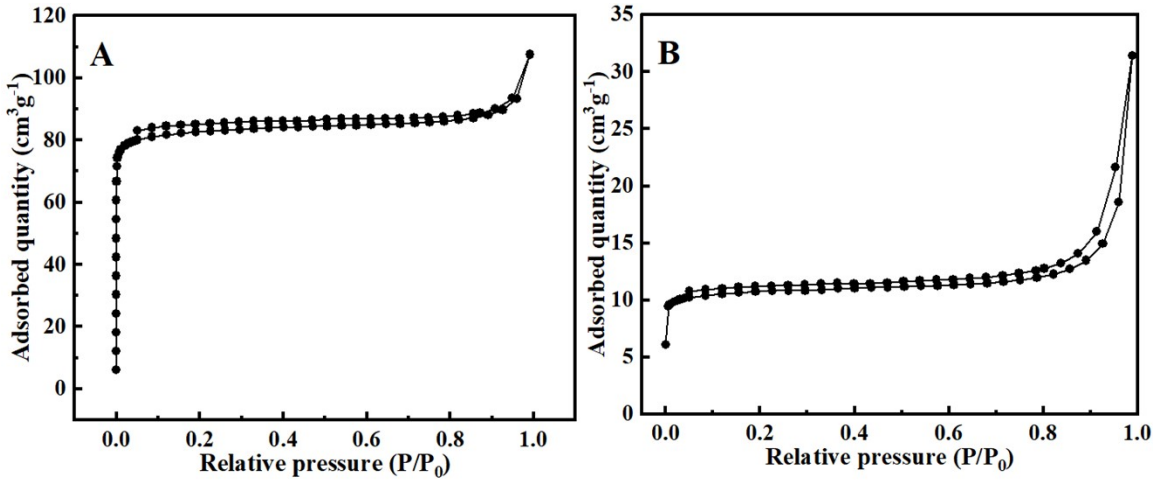


**Fig. S15.** $N_2$ sorption isotherms of K-GME (A) and T-GME (B) samples.

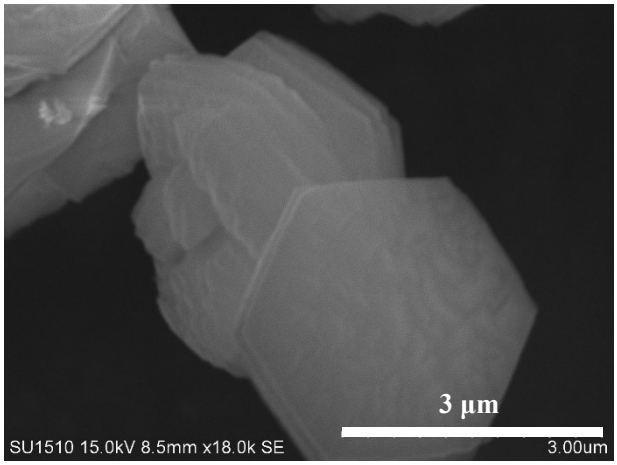


**Fig. S16.** SEM image of T-GME zeolite with faults synthesized by interzeolite transformation.

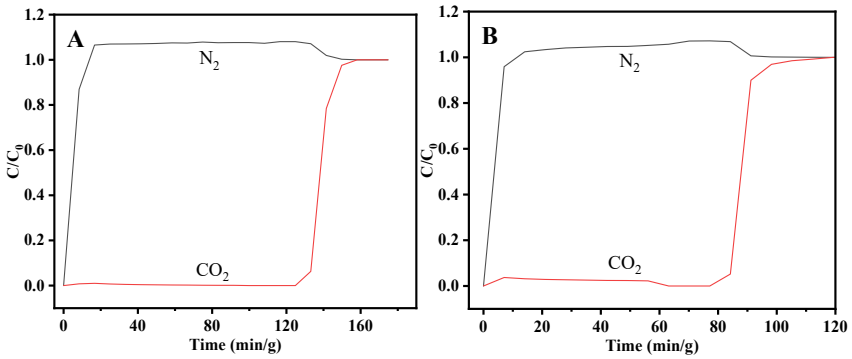


**Fig. S17.** $CO_2/N_2$ (15/85, v/v) mixture breakthrough curves of K-GME(A) and T-GME(B) samples.

**Table S1.** Micropore volumes and BET surface of GME samples

| Type of GME | $V_{micro}(cm^3/g)$ | $V_{total}(cm^3/g)$ | $S_{BET}(m^2/g)$ |
|---|---|---|---|
| Na-GME | 0.16 | 0.21 | 341 |
| K-GME | 0.12 | 0.17 | 255 |
| T-GME | 0.02 | 0.05 | 33 |

**Table S2.** Adsorption capacity and $CO_2$ selectivity for different types of zeolites at 1 bar and 25 °C

| Zeolite | $CO_2$(mmol/g) | Selectivity[a] | Ref. |
|---|---|---|---|
| Na-GME | 5.4 | 58.8 | This work |
| Na-BEA | 2.7 | 16.8 | 1 |
| Fe-MOR | 3.9 | 51.8 | 2 |
| Na-PST-29 | 4.3 | 30 | 3 |
| K-MER-2.3 | 2.9 | 64 | 4 |
| 2K-SSZ-13 | 4.8 | 50 | 5 |

[a] Selectivities measured from $CO_2/N_2$ (0.15/0.85) mixture.

## References:


[1] S. T. Yang, J. Kim and W. S. Ahn, *Microporous Mesoporous Mater*., 2010, **135**, 90-94.

[2] Y. Zhou, J. L. Zhang, L. Wang, X. L. Cui, X. L. Liu, S. S. Wong, H. An, N. Yan, J. Y. Xie, C. Yu, P. X. Zhang, Y. H. Du, S. B. Xi, L. R. Zheng, X. Z. Cao, Y. J. Wu, Y. X. Wang, C. Q. Wang, H. M. Wen, L. Chen, H. B. Xing and J. Wang, *Science*, 2021, **373**, 315-320.

[3] H. Lee, J. Shin, W. Choi, H. J. Choi, T. M. Yang, X. D. Zou and S. B. Hong, *Chem. Mater.,* 2018, **30**, 6619-6623.

[4] H. J. Choi, D. Jo, J. G. Min and S. B. Hong, *Angew. Chem. Int. Ed.,* 2021, **60**, 4307-4314.

[5] J. K. Bower, D. Barpaga, S. Prodinger, R. Krishna, H. T. Schaef, B. P. McGrail, M. A. Derewinski and R. K. Motkuri, *ACS Appl. Mater. Interfaces,* 2018, **10**, 14287-14291.